

Non-linear dispersive regime of circuit QED: The dressed dephasing model

Maxime Boissonneault,¹ Jay Gambetta,^{2,3} and Alexandre Blais¹

¹*Département de Physique et Regroupement Québécois sur les Matériaux de Pointe, Université de Sherbrooke, Sherbrooke, Québec, Canada, J1K 2R1*

²*Institute for Quantum Computing and Department of Physics and Astronomy, University of Waterloo, Waterloo, Ontario N2L 3G1, Canada*

³*Centre for Quantum Computer Technology, Centre for Quantum Dynamics, Griffith University, Brisbane, Queensland 4111, Australia*

(Dated: January 26, 2023)

In the dispersive limit of circuit quantum electrodynamics, the signal-to-noise ratio (SNR) was predicted to scale linearly with photon population of the resonator. However, experiments have rather shown saturation of the SNR. We present a model which takes into account dressing of the qubit by the photons to explain this behavior. It also suggests how to optimize the SNR. We find that in the presence of pure qubit dephasing, photons used for measurement of the qubit act as a heat bath, inducing incoherent relaxation and excitation of the qubit. Measurement thus induces both dephasing and mixing of the qubit, reducing the quantum non-demolition aspect of the readout.

Coupling of mesoscopic systems to quantum oscillators is a very active field opening new parameter regimes for quantum optics. Examples of realizations of quantum optics on a chip are the active cooling of a nanomechanical [1] or electromagnetic [2] oscillators by use of superconducting circuits. Another example is circuit quantum electrodynamics (QED) where a superconducting charge qubit is fabricated inside a transmission line resonator [3]. This system, which is an on-chip realization of cavity QED, was shown to reach the strong-coupling regime [4] and more recently the novel strong *dispersive* regime [5].

In circuit QED, the Hamiltonian and parameters describing the qubit and resonator can be known with very good accuracy allowing for quantitative comparison of experimental results to theoretical expectations. However, one prediction which so far has not been realized experimentally is the possibility of having large signal-to-noise ratio (SNR) in measurement of the qubit by homodyne detection of the resonator voltage. Indeed, one would expect the SNR achievable in an integration time set by the qubit relaxation time T_1 to simply be proportional to the number of photons populating the resonator [3, 6]. As a result, by increasing the photon population, very large SNR's should be realizable. In practice however, the SNR has rather been limited to $\lesssim 5$ [7]. Larger values would allow rapid and faithful qubit state readout [8], something that is critical for quantum information processing and which also opens the possibility to probe in more details the very rich physics of these driven and damped oscillator-qubit systems.

In this letter, by studying the qubit-resonator Hamiltonian in the higher-order dispersive regime, we find a mechanism that can explain the reduction of the SNR in circuit QED. In addition to gaining insights on the problem of the low SNR, we obtain a simple effective master equation that describes with very high accuracy the qubit dynamics in the presence of measurement. A stochastic master equation, or quantum trajectory equation [9], taking into account the act of measurement on the system is also presented.

Circuit QED is described by the Jaynes-Cummings hamiltonian

$$H_s = \hbar\omega_r a^\dagger a + \hbar\omega_a \frac{\sigma_z}{2} + \hbar g (a^\dagger \sigma_- + a \sigma_+), \quad (1)$$

where $a^{(\dagger)}$ and σ_\pm are ladder operators for the photon field and the qubit respectively, ω_r the resonator frequency, ω_a the qubit transition frequency and g the qubit-resonator coupling strength. Readout of the qubit is realized by populating the resonator with a coherent field and measuring the transmitted signal in a homodyne measurement. For this purpose, a coherent drive on the resonator is modeled by the hamiltonian $H_d = \hbar\epsilon_m(t) (a^\dagger e^{-i\omega_m t} + a e^{i\omega_m t})$, with $\epsilon_m(t)$ and ω_m the measurement amplitude and frequency, respectively.

Energy relaxation is modeled by coupling the resonator and qubit to baths of harmonic oscillators [9]

$$H_j = i\hbar \int_0^\infty \sqrt{g_j(\omega)} [b_j^\dagger(\omega) - b_j(\omega)] [c_j^\dagger + c_j] d\omega, \quad (2)$$

where $j = \kappa$ or γ representing either the resonator or the qubit baths, with $c_\kappa = a$ and $c_\gamma = \sigma_-$. Here, $g_j(\omega)$ represents the coupling strength to the bath mode of frequency ω . In the Born-Markov approximation, integrating out the baths leads to a qubit-resonator master equation of Lindblad form characterized by the resonator decay rate $\kappa = 2\pi|g_\kappa(\omega_r)|^2$ and qubit relaxation rate $\gamma_1 = T_1^{-1} = 2\pi|g_\gamma(\omega_a)|^2$. Qubit dephasing can be modeled by coupling to a longitudinal classical fluctuating force $f(t)$ using the Hamiltonian $H_\varphi = \hbar v f(t) \sigma_z$, where v is characteristic of the magnitude of the coupling of the qubit to the fluctuations. This leads to pure dephasing of the qubit at a rate $\gamma_\varphi = 2v^2 S_f(\omega \rightarrow 0)$, with $S_f(\omega)$ the noise spectrum of $f(t)$.

In this letter, we focus on the dispersive regime of cavity, or circuit, QED which is relevant for qubit measurement. Namely, we will always take the detuning $|\Delta| \equiv |\omega_a - \omega_r|$ between the qubit and the resonator to be much larger than the coupling g . In this situation,

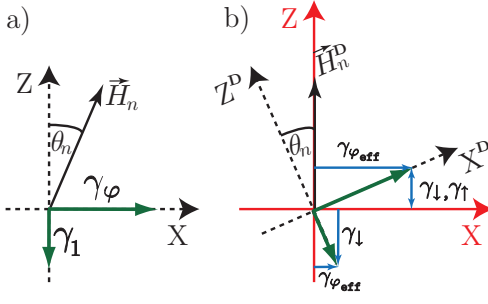


FIG. 1: (Color online) Geometrical representation of the Jaynes-Cummings Hamiltonian in \mathcal{E}_n with decay and dephasing rates for a) the bare and b) dispersive basis. The axes X^D and Z^D are the original axes which were rotated by an angle $\theta_n = \arctan(2\lambda\sqrt{n})$ around the Y axis such that H^D is along the Z direction.

it is useful to go to the dispersive basis by using a unitary transformation to diagonalize Eq. (1). This is done using $\mathbf{D} = \exp[\Lambda(N_q)(a^\dagger\sigma_- - a\sigma_+)]$, where $\Lambda(N_q) = -\arctan(2\lambda\sqrt{N_q})/2\sqrt{N_q}$ and $N_q \equiv a^\dagger a + |e\rangle\langle e|$ is an operator representing the total number of excitations. While this can be done exactly, here we only present the result to third order in the small parameter $\lambda = g/\Delta$

$$\begin{aligned} H_s^D &= \mathbf{D}H_s\mathbf{D}^\dagger \\ &\approx \hbar(\omega_r + \zeta)a^\dagger a + \hbar\left[\omega_a + 2\chi\left(a^\dagger a + \frac{1}{2}\right)\right]\frac{\sigma_z}{2} \\ &\quad + \hbar\zeta(a^\dagger a)^2\sigma_z, \end{aligned} \quad (3)$$

where $\chi = g^2(1 - \lambda^2)/\Delta$ is the Stark shift per photon. This Hamiltonian is similar to the usual dispersive Hamiltonian [3], but the third order expansion leads to corrections to χ , to the resonator frequency and also yields a squeezing term $(a^\dagger a)^2$ of amplitude $\zeta = -g^4/\Delta^3$.

The transformation \mathbf{D} to the dispersive basis can be interpreted as a rotation in the qubit-resonator space. To see this more explicitly and as a way to understand how this transformation will affect dissipation, it is useful to consider the subspace $\mathcal{E}_n = \{|n+1, g\rangle, |n, e\rangle\}$. In \mathcal{E}_n , H_s takes the form $H_s^n = \hbar\Delta\bar{\sigma}_z/2 + \hbar g\sqrt{n}\bar{\sigma}_x$, where $\bar{\sigma}_{x,z}$ act as Pauli operators on \mathcal{E}_n . As illustrated in Fig. 1, this Hamiltonian is diagonalized by a rotation about the y axis of angle $\theta_n = \arctan(2\lambda\sqrt{n})$. The second order dispersive approximation simply corresponds to taking $\theta_n \approx 2\lambda\sqrt{n}$. On the other hand, the exact transformation \mathbf{D} corresponds to performing the above rotation in all subspaces $\mathcal{E}_{n>0}$. After this transformation, the new eigenstates are entangled superpositions of qubit and resonator states. Hence, in the dispersive basis, the qubit acquires a photon part and vice versa.

In addition to the system Hamiltonian, it is also important to rotate the system-bath Hamiltonians. As illustrated in Fig. 1, representing the qubit relaxation rate γ_1 by an arrow pointing along the original axis z^D , once rotated it acquires a component along the x axis corresponding to dephasing. Relaxation also sees its compo-

nent along the z reduced in magnitude. In the same way, dephasing pointing along x^D acquires a component along z corresponding to upward and downward transitions of the qubit, while also reducing in magnitude along x . Since the rotation angle θ_n varies with n , from this simple picture we therefore expect the effective qubit decay and dephasing rates to depend on the subspace \mathcal{E}_n and therefore on the number of photons in the cavity.

To obtain an effective master equation for the qubit in the third order dispersive approximation, we therefore apply the transformation \mathbf{D} to the system-bath Hamiltonians as well as to the drive Hamiltonian H_d . The baths are then integrated out to obtain Lindblad form dissipators for the qubit and resonator operators [9]. Starting from this transformed master equation, our goal is to obtain an effective master equation for the qubit only. To arrive at this result, we follow Ref. [6] in tracing out the resonator degrees of freedom by first applying a polaron-type transformation to the qubit-resonator master equation. While in the linear dispersive approximation this results in an exact qubit master equation [6], in the non-linear case we approximate the photon number operator $a^\dagger a$ by linearizing quantum fluctuations around the classical value. In this way, we obtain the following master equation for the qubit density matrix ρ^D in the dispersive basis

$$\begin{aligned} \dot{\rho}^D &= -i\frac{\tilde{\omega}_a^D}{2}[\sigma_z, \rho^D] + \frac{\gamma_{\varphi\text{eff}}}{2}\mathcal{D}[\sigma_z]\rho^D \\ &\quad + \gamma_\downarrow\mathcal{D}[\sigma_-]\rho^D + \gamma_\uparrow\mathcal{D}[\sigma_+]\rho^D. \end{aligned} \quad (4)$$

In this expression, $\tilde{\omega}_a^D$ is the Lamb and Stark shifted qubit transition frequency, including both linear [6] and quadratic in photon number (i.e. squeezing) contributions. The effective dephasing rate $\gamma_{\varphi\text{eff}}$ takes into account measurement-induced dephasing [10] and its non-linear contribution. In this letter, we focus on the effective decay and excitation rates and only present these terms explicitly. They are given by

$$\gamma_\downarrow = \gamma_1 \left[1 - \frac{2\bar{n} + 1}{4n_{\text{crit}}}\right] + \gamma_\kappa + \gamma_\Delta\bar{n} \quad (5a)$$

$$\gamma_\uparrow = \gamma - \Delta\bar{n}, \quad (5b)$$

where $\gamma_\kappa = 2\pi|g_\kappa(\omega_a)|^2/4n_{\text{crit}}$ is the Purcell decay rate and $\gamma_{\pm\Delta} = v^2 S_f(\pm\Delta)/n_{\text{crit}}$ are measurement and dephasing induced heating and relaxation rates. In these expressions $n_{\text{crit}} = \Delta^2/4g^2$ is the critical photon number [3] and $\bar{n} = P_g n_g + P_e n_e$ is the average number of photons in the resonator, with $P_{g,e}$ the ground and excited population and $n_{g,e} = |\alpha_{g,e}|^2$ the photon population corresponding to the classical fields $\alpha_{g,e}$ associated to the qubit ground and excited states. These satisfy

$$\begin{aligned} \dot{\alpha}_{g,e} &= -i[\Delta'_{rm} \mp \delta_{g,e}]\alpha_{g,e} - i\epsilon_m \left[1 \mp \frac{1}{8n_{\text{crit}}}\right] \\ &\quad - \frac{\kappa}{2} \left[1 \mp \frac{1}{4n_{\text{crit}}}\right] \alpha_{g,e}, \end{aligned} \quad (6)$$

where $\Delta'_{rm} = \omega_r - \omega_m + \zeta$ is the rotating-frame resonator frequency and $\delta_{g,e} = \chi + 2\zeta n_{g,e}$ the resonator pull.

As discussed in relation to the geometrical picture of Fig. 1, we see that in the dispersive picture, the qubit relaxation rate can be reduced by photon population [negative sign in Eq. (5a)]. Since in the dispersive basis the qubit is dressed by the photons, and that this dressing increases with \bar{n} , it must be less sensitive to noise at the qubit transition frequency with increasing \bar{n} . However, the relaxation rate is now enhanced by noise at the detuning frequency. In the same way, the qubit acquires a finite excitation rate γ_{\uparrow} . We thus see that dressing of dephasing leads to the measurement photon acting as a heat bath for the qubit. Numerical calculations have shown this effective master equation to accurately capture the dynamics of the qubit up to photon population of the order of n_{crit} for the parameters used in Fig. 2.

Under continuous observation of the photons leaving the resonator, the above description does not take into account the results of our observation and is therefore incomplete. To take into account this information and calculate the expected SNR we use quantum trajectory theory [6, 9, 11] to derive the evolution equation for the conditional state. This was done in Ref. [6] for the linear dispersive model and is extended here to take into account the non-linear effects. For phase measurement (i.e. homodyne detection of the ϕ -quadrature [11]), we find that the state of the qubit conditioned on the record $\bar{J}(t)$ obeys the stochastic master equation (SME)

$$\begin{aligned} \dot{\rho}_J^{\mathbf{D}} = & \mathcal{L}^{\mathbf{D}} \rho_J^{\mathbf{D}} + \sqrt{\Gamma_{\text{ci}}(t)} \mathcal{M}[\sigma_z] \rho_J^{\mathbf{D}}(t) (\bar{J}(t) - \sqrt{\Gamma_{\text{ci}}(t)} \langle \sigma_z \rangle_t) \\ & - i \frac{\sqrt{\Gamma_{\text{ba}}(t)}}{2} [\sigma_z, \rho_J^{\mathbf{D}}(t)] (\bar{J}(t) - \sqrt{\Gamma_{\text{ci}}(t)} \langle \sigma_z \rangle_t) \end{aligned} \quad (7)$$

where $\mathcal{L}^{\mathbf{D}} \cdot$ is given by Eq. (4) and $\mathcal{M}[c]\varrho = (c - \langle c \rangle_t)\varrho/2 + \varrho(c - \langle c \rangle_t)/2$, is the measurement superoperator with $\langle c \rangle_t = \text{Tr}[c\rho_J^{\mathbf{D}}(t)]$. The measurement results $\bar{J}(t)$ is $\bar{J}(t) = \sqrt{\Gamma_{\text{ci}}(t)} \langle \sigma_z \rangle_t + \xi(t)$, where $\xi(t)$ is Gaussian white noise satisfying $E[\xi(t)] = 0$ and $E[\xi(t)\xi(t')] = \delta(t - t')$.

The SME (7) is of Itô form and represents a gradual projective measurement of σ_z . The rate at which information about the state of the qubit comes out of the resonator (the coherent information) is given by

$$\Gamma_{\text{ci}}(t) = \eta \Gamma_m \cos^2(\theta_m) \quad (8)$$

where

$$\Gamma_m = \kappa |\beta|^2 \left(1 + \frac{|\mu| \cos(\theta_\beta - \theta_\mu)}{4|\beta|n_{\text{crit}}} + \frac{|\mu|^2}{64|\beta|^2 n_{\text{crit}}^2} \right), \quad (9a)$$

$$\theta_m = \phi - \theta_\beta + \text{Im} \left\{ \log \left[1 + \frac{|\mu| e^{i(\theta_\beta - \theta_\mu)}}{8|\beta|n_{\text{crit}}} \right] \right\}, \quad (9b)$$

with $\beta = \alpha_e - \alpha_g$, $\mu = \alpha_e + \alpha_g$ and the angles $\theta_\beta = \arg(\beta)$, $\theta_\mu = \arg(\mu)$. For clarity of presentation, the above expression for Γ_m has been simplified such that it is only valid for $\phi - \theta_\beta \in [0, \pi/2]$. Furthermore, η is a detection efficiency parameter. Choosing the reference phase ϕ (the

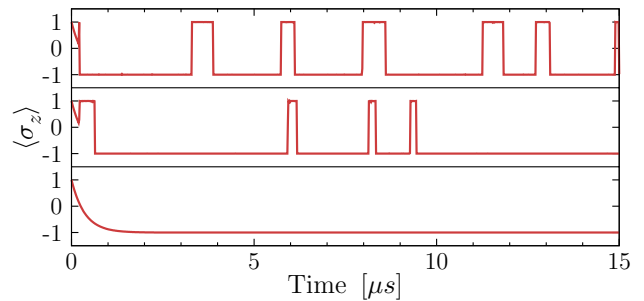


FIG. 2: (Color online) Typical trajectories for measurement amplitudes $\epsilon_m/2\pi = 0$ MHz (bottom), 50 MHz (center) and 80 MHz (top). The parameters used are $(\omega_a - \omega_r)/2\pi = 1.7$ GHz, $g/2\pi = 170$ MHz, $\kappa/2\pi = 34$ MHz, $\gamma_{\uparrow}/2\pi = 0.1$ MHz, $\gamma_{\pm\Delta} = 2\lambda^2\gamma_{\varphi}$ with $\gamma_{\varphi}/2\pi = 0.1$ MHz and $\eta = 1$. These parameters correspond to $n_{\text{crit.}} = 25$. The initial state has $\langle \sigma_z \rangle = 1$ with zero photons and a measurement drive starting shortly after $t = 0$.

phase of the local oscillator) such that $\theta_m = 0$, the rate of information gain about the qubit state is $\eta\Gamma_m$. To first order in λ , this can be simply understood by noting that $\eta\kappa$ is the rate at which photons leak out the resonator and are detected, while $|\beta|^2$ is the amount of information about the qubit state encoded in the photons. The second order term in Γ_m is a correction arising from the fact that, in the dispersive frame, the qubit is dressed by the photon. Finally, the rate $\Gamma_{\text{ba}}(t) = \eta\Gamma_m \sin^2(\theta_m)$ in the SME, represents extra non-Heisenberg back-action due to the measurement. This rate is zero when $\theta_m = 0$ and is maximum when measuring in the opposite quadrature.

Typical trajectories obtained by numerical integration of the SME are shown in Fig. 2 for three different measurement amplitudes ϵ_m . In the linear dispersive model, as the measurement amplitude is increased the qubit state localizes on one of the basis states [6]. If this localization is faster than the relaxation time γ_{\uparrow}^{-1} , then the measurement result is a faithful representation of the initial qubit state. However, and in contrast to the predictions from the linear dispersive model, in the large measurement power limit we do not expect a single jump to the ground state to occur with mean jump time $1/\gamma_{\uparrow}$. Instead telegraph noise due to the measurement induced excitation rate γ_{\uparrow} is expected. These predictions can be experimentally tested by measuring the waiting time between jumps and comparing to γ_{\uparrow} and γ_{\downarrow} .

As is clear from the above results, increasing the measurement amplitude opens a new mixing channel γ_{\uparrow} which leads to a loss of the quantum non-demolition (QND) character of the dispersive measurement. As a result, and contrary to initial expectations [3, 6], we therefore expect the SNR to saturate with increasing measurement power. To demonstrate this in the situation where bifurcation [12] is not important, we define the SNR as $\text{SNR} = (\text{SNR}_e + \text{SNR}_g)/2$ where

$$\text{SNR}_{e(g)} = \Gamma_{\text{ci}} / (\gamma_{\uparrow e(g)} + \gamma_{\downarrow e(g)}) \quad (10)$$

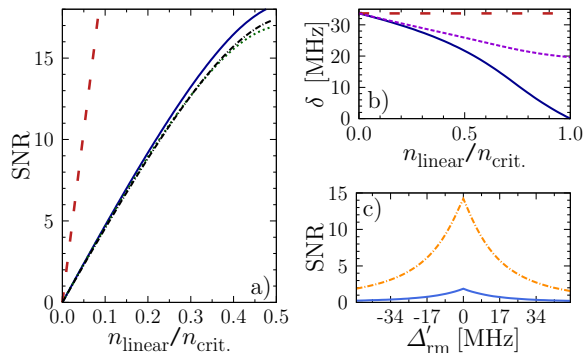


FIG. 3: (Color online) a) SNR vs $n_{\text{linear}}/n_{\text{crit}}$ for $\Delta'_{rm} = 0$ in the linear (dashed red) and second order (full blue) models. Dotted green is Eq. (11). Dashed-dotted black includes transients. b) Cavity pull δ vs $n_{\text{linear}}/n_{\text{crit}}$ in the linear model (dashed red), second order approximation (full blue) and exact (dotted purple). c) SNR vs measurement detuning Δ'_{rm} at fixed photon population (dashed-dotted orange $n = 10$, full blue $n = 1$). Parameters are the same as in Fig. 2 and $\eta = 1/80$ consistent with experimental observations [7].

is the SNR for the qubit initially in the excited (ground) state. The rates $\gamma_{\uparrow e(g)}$ and $\gamma_{\downarrow e(g)}$ depend on the qubit state through the photon population which is evaluated from the steady-state value of Eq. (6).

Fig. 3a) shows a plot of the SNR (solid blue) as a function of measurement power ϵ_m^2 and scaled to $n_{\text{linear}}/n_{\text{crit}}$ where $n_{\text{linear}} = \epsilon_m^2/(\kappa^2/4 + \chi^2)$ is the average photon number predicted by the linear model. Contrary to the result obtained in the linear model (dotted red), the SNR is seen to saturate with increasing power. For κ/γ_1 small, transients can further reduce the SNR. For the chosen parameters (dashed-dotted black) this reduction is small. The value at saturation is within a factor of two or three of that observed experimentally [7] for a transmon qubit [13]. At fixed g, χ for the transmon is reduced substantially by the presence of extra qubit levels with respect to the two-level system (Cooper pair box) studied here, resulting in a lower SNR. Along with the fact that η is highly dependent on parameters that are difficult to extract experimentally (e.g. number of thermal photons produced by the leading amplifier), the agreement with theory is excellent.

The saturation of the SNR is due to the increase in $\gamma_{\uparrow} + \gamma_{\downarrow}$ and to a reduction of the cavity pull with photon number. While numerical simulations have shown the re-

duced dispersive master equation (4) to be very accurate to about $n_{\text{crit}} \sim 25$ photons, as shown in Fig. 3b), cavity pull in the non-linear model (full blue) starts to deviate significantly from the exact result obtain from diagonalization of the Jaynes-Cummings Hamiltonian (dashed green) at about $n_{\text{crit}}/2 \sim 13$. Our prediction for the SNR therefore underestimate slightly the exact result in the range shown in Fig. 3a).

Moreover, as shown in Fig. 3c), the SNR is maximized by choosing a measurement frequency such that $\Delta'_{rm} = 0$. This value was used in Fig. 3a). For this optimal detuning and assuming that $O(n_{\text{crit}}^{-1})$ terms can be neglected in Eqs. (6) and (9), we find

$$\text{SNR} \approx \frac{4\eta\kappa(\chi + 2\zeta n)^2}{[\kappa^2/4 + (\chi + 2\zeta n)^2][\gamma_{\uparrow} + \gamma_{\downarrow}]}, \quad (11)$$

where we have taken $\phi = \theta_{\beta}$. This is shown as the green dashed line in Fig. 3a) where it is seen to be a very good approximation at low power.

Using these results, it is possible to find parameters that maximize the SNR. For example, for a given value of n/n_{crit} one can find an optimal value of κ . If $\gamma_{\uparrow} + \gamma_{\downarrow}$ was independent of n , we find from Eq. (11) that the optimal value would be $\kappa_{\text{opt}}/2 = (\chi + 2\zeta n)$ which depends on power. In general, it will also depend on the relaxation γ_1 and dephasing γ_{ϕ} rates. In the case where $\gamma_{\phi} \approx \gamma_1$, the optimal κ is approximately κ_{opt} as $\gamma_{\uparrow} + \gamma_{\downarrow}$ is only weakly dependent on n , while when dephasing dominates over relaxation the optimal κ increases with power in order to limit the photon population and thus unwanted qubit mixing. Clearly, dephasing plays an important role in the reduction of the SNR and is therefore a crucial parameter to suppress. Efforts in this direction [13] have already paid off [14], something which is promising in light of the current results.

In summary, we have shown that under measurement a qubit coupled to a resonator will suffer from additional mixing due to the, a priori QND, coupling to the resonator. This leads to a reduction of the SNR consistent with experimental observations. The current results offer an approach to optimize the SNR in the ubiquitous qubit-harmonic oscillator system.

We thank A. A. Houck, R. J. Schoelkopf and S. M. Girvin for discussions. MB was supported by NSERC, AB by NSERC, FQRNT, CIFAR and JG by MITACS, ORDCF, Australian Research Council (CE0348250), and the State of Queensland.

[1] A. Naik, O. Buu, M. D. LaHaye *et al*, Nature **443**, 193 (2006).
 [2] M. Grajcar, S. van der Ploeg, A. Izmalkov *et al*, arXiv:0708.0665v1 (2007).
 [3] A. Blais, R.-S. Huang, A. Wallraff *et al*, Phys. Rev. A **69**, 062320 (2004).
 [4] A. Wallraff, D. I. Schuster, A. Blais *et al*, Nature **431**,

162 (2004).
 [5] D. I. Schuster, A. A. Houck, J. A. Schreier *et al*, and R. J. Schoelkopf, Nature **445**, 515 (2007).
 [6] J. Gambetta, A. Blais, M. Boissonneault *et al*, Phys. Rev. A **77**, 012112 (2008).
 [7] A. A., Houck, B. R. Jonhson and R. J. Schoelkopf, private communication.

- [8] J. Gambetta, W. A. Braff, A. Wallraff *et al*, Phys. Rev. A **76**, 012325 (2007).
- [9] H. J. Carmichael, *An Open System Approach to Quantum Optics* (Springer, Berlin, 1993).
- [10] J. Gambetta, A. Blais, D. I. Schuster *et al*, Phys. Rev. A **74**, 042318 (2006).
- [11] H. M. Wiseman and G. J. Milburn, Phys. Rev. A **47**, 642 (1993).
- [12] I. Siddiqi, R. Vijay, F. Pierre *et al*, Phys. Rev. Lett. **93**, 207002 (2004).
- [13] J. Koch, T. M. Yu, J. Gambetta *et al*, Phys. Rev. A **76**, 042319 (2007).
- [14] J. A. Schreier, A. A. Houck, J. Koch *et al*, arXiv:0712.3581 (2007).